

On the maximum principle and energy stability for fully discretized fractional-in-space Allen-Cahn equation

Tianliang Hou* Tao Tang † Jiang Yang ‡

November 23, 2013

Abstract

We consider numerical methods for solving the fractional-in-space Allen-Cahn (FiSAC) equation which contains small perturbation parameters and strong nonlinearity. Standard fully discretized schemes for the the FiSAC equation will be considered, namely, in time the conventional first-order implicit-explicit scheme or second-order Crank-Nicolson scheme and in space a second-order finite difference approach. The main purpose of this work is to establish discrete stability in both *maximum* and energy norms. In particular, we will show that the numerical results obtained by using the fully discretized schemes are conditionally stable: both the discrete maximum principle and the energy decaying properties are preserved under certain restrictions on the time step. Moreover, our analysis applied to one to three space dimensions. Numerical experiments are performed to verify the theoretical results.

Key Words. Fractional-in-space, Allen-Cahn equations, finite difference method, maximum principle, energy stability.

*Research Institute of Hong Kong Baptist University in Shenzhen, Shenzhen 518057, Guangdong, China & Huanan Normal University ... Email: htlchb@163.com.

†Corresponding author. Institute of Theoretical and Computational Studies & Department of Mathematics, Hong Kong Baptist University, Kowloon Tong, Hong Kong. Email: ttang@hkbu.edu.hk.

‡Department of Mathematics, Hong Kong Baptist University, Kowloon Tong, Hong Kong. Email: jyanghkbu@gmail.com.

1 Introduction

In this paper, we study the numerical approximations to the fractional-in-space Allen-Cahn equation (FiSAC)

$$\frac{\partial u}{\partial t} = -\epsilon^2(-\Delta)^{\frac{\alpha}{2}}u - f(u), \quad \mathbf{x} \in \Omega, t \in (0, T], \quad (1.1)$$

$$u(\mathbf{x}, 0) = u_0(\mathbf{x}), \quad \mathbf{x} \in \bar{\Omega}, \quad (1.2)$$

$$u|_{\partial\Omega} = 0, \quad (1.3)$$

where Ω is a bounded regular domain in R^d ($d = 1, 2, 3$), $\alpha \in (1, 2)$, and the nonlinear source term is taken as the same as in the standard Allen-Cahn equation. The fractional Laplacian operator in one-space dimension is defined by the Riesz fractional derivative

$$-(-\Delta)^{\frac{\alpha}{2}}u = -(-\Delta)_x^{\frac{\alpha}{2}}u := \frac{1}{-2 \cos \frac{\pi\alpha}{2}}({}_aD_x^\alpha u + {}_xD_b^\alpha u), \quad (1.4)$$

where the left and right Riemann-Liouville fractional derivatives are defined as

$${}_aD_x^\alpha u = \frac{1}{\Gamma(2-\alpha)} \frac{d^2}{dx^2} \int_a^x \frac{u(\xi)}{(x-\xi)^{\alpha-1}}, \quad (1.5)$$

$${}_xD_b^\alpha u = \frac{1}{\Gamma(2-\alpha)} \frac{d^2}{dx^2} \int_x^b \frac{u(\xi)}{(x-\xi)^{\alpha-1}}. \quad (1.6)$$

The fractional Laplacian operators in 2D and 3D can be defined similarly. For example, the 3D operator is defined as

$$-(-\Delta)^{\frac{\alpha}{2}}u(x, y, z) = \left\{ \left[-(-\Delta)_x^{\frac{\alpha}{2}} \right] + \left[-(-\Delta)_y^{\frac{\alpha}{2}} \right] + \left[-(-\Delta)_z^{\frac{\alpha}{2}} \right] \right\} u(x, y, z). \quad (1.7)$$

Fractional models, in which a standard time or space differential operator is replaced by a corresponding fractional differential operator, have a long history in, for example, physics, finance and hydrology, with such models often being used to represent so-called anomalous diffusion. As the analytical solutions can not be obtained, there have been increasing efforts in studying numerical methods for solving the fractional differential equations. For the time fractional problems, finite difference schemes and spectral methods have been investigated, see, e.g., [9–11].

In recent years, there has been tremendous interest in using the diffusive-interface phase-field approach for modeling the mesoscale morphological pattern formation and interface motion. One of the very effective mathematical models describing these physical phenomena is the Allen-Cahn

equation introduced in 1979 [1]. Roughly speaking, the Allen-Cahn equation describes regions with $u \approx 1$ and $u \approx -1$ that grow and decay at the expense of one another. As the governing equations are nonlinear, many numerical works have been devoted to the solutions of the Allen-Cahn equation, see, e.g., [?, 3–7, 14, 17, 19]. The key indicators for numerical solutions are high stability and accuracy, which yield the requirement of small time step and spatial grid size. However, this requirement seriously limits the system size and the length of the simulation time. As reliable performance of the phase-field computations demands long simulation time, it is critical to understand the stability properties of the underlying numerical schemes. One of the intrinsic properties of the Allen-Cahn equation is that the energy function is decreasing with time. In the past two decades, the numerical stability has been mostly restricted to this energy decreasing property. This is in particular becoming popular due to the convex-concave splitting idea of Eyre [4]. Very recently, Tang and Yang [16] established a stability criteria in a stronger sense.

It is noted that the combination of the fractional model and the Allen-Cahn model, namely, the fractional-in-space Allen-Cahn equation (1.1), is a challenging mathematical and numerical problem. It has attracted attentions in recent years. For problem (1.1), Burrage et al. [2] proposed an efficient implicit finite element scheme, Bueno-Orovio et al. [12] considered the Fourier spectral methods. Zhuang et al. [20] considered the finite difference method for fractional-in-space reaction diffusion equation with a nonlinear source term that satisfies the Lipschitz condition.

The main result in [16] is that the finite difference solutions of the Allen-Cahn equation satisfies the maximum principle in the sense that if their initial data is bounded by 1 then the numerical solutions in later times can also be bounded uniformly by 1. In this work, we wish to see if this maximum principle still holds for the numerical solutions of the FiSAC equation (1.1). To this end, we consider a couple of standard fully discretized schemes for (1.1), i.e., we use the first-order implicit-explicit scheme or second-order Crank-Nicolson scheme in time and the second-order finite difference approximation in space. The main targets of this work are of two folds. First, we will prove that the numerical solutions will satisfy the maximum principle in the sense mentioned above. Secondly, we will show that the discrete energy of the numerical solutions decay with time.

The rest of the paper is organized as follows. In Section 2, fully discretized schemes to approximate the FiSAC equation (1.1) will be provided. The stability in the maximum-norm and in the

energy norm will be established in Sections 3 and 4, respectively. In Section 5, some numerical examples are carried out to illustrate the theoretical results and some concluding remarks will be given in the last section.

2 The fully discretized schemes

We will adopt the finite difference approach in [15] to discretize the fractional Laplacian operator $-(-\Delta)^{\frac{\alpha}{2}}$. To begin with, we denote D_h as the discrete matrix of the fractional Laplacian operator. In particular, the discrete matrix of ${}_a D_x^\alpha$ with homogeneous Dirichlet boundary conditions on interval $[0, L]$ in one-space dimension is given by

$$A = \frac{1}{h^\alpha} \begin{bmatrix} \omega_1^{(\alpha)} & \omega_0^{(\alpha)} & & & & \\ \omega_2^{(\alpha)} & \omega_1^{(\alpha)} & \omega_0^{(\alpha)} & & & \\ \vdots & \omega_2^{(\alpha)} & \omega_1^{(\alpha)} & \ddots & & \\ \omega_{N-1}^{(\alpha)} & \dots & \ddots & \ddots & \omega_0^{(\alpha)} & \\ \omega_N^{(\alpha)} & \omega_{N-1}^{(\alpha)} & \dots & \omega_2^{(\alpha)} & \omega_1^{(\alpha)} & \end{bmatrix}_{N \times N} =: \frac{1}{h^\alpha} M,$$

where

$$\begin{aligned} \omega_0^{(\alpha)} &= \frac{\alpha}{2}, \quad \omega_1^{(\alpha)} = \frac{2-\alpha-\alpha^2}{2} < 0, \quad \omega_2^{(\alpha)} = \frac{\alpha(\alpha^2-\alpha-4)}{4}, \\ 1 \geq \omega_0^{(\alpha)} &\geq \omega_3^{(\alpha)} \geq \omega_4^{(\alpha)} \geq \dots \geq 0, \quad \sum_{k=0}^{\infty} \omega_k^{(\alpha)} = 0, \end{aligned} \quad (2.8)$$

and h is the mesh size in space. Note that the discrete matrix of ${}_x D_b^\alpha$ is A^T . Defining

$$D = M + M^T \quad (2.9)$$

produces the discrete matrix of the fractional Laplacian operator in one-space dimension:

$$D_h^{(1)} = \frac{1}{-2h^\alpha \cos \frac{\pi\alpha}{2}} D. \quad (2.10)$$

Using the Kronecker tensor product notation, we can obtain the corresponding discrete matrix in two space dimension

$$D_h^{(2)} = \frac{1}{-2h^\alpha \cos \frac{\pi\alpha}{2}} (I \otimes D + D \otimes I), \quad (2.11)$$

where I is the $N \times N$ identity matrix. Similarly, the discrete matrix in three space dimension can be represented as

$$D_h^{(3)} = \frac{1}{-2h^\alpha \cos \frac{\pi\alpha}{2}} (I \otimes I \otimes D + I \otimes D \otimes I + D \otimes I \otimes I). \quad (2.12)$$

We close this section by describing our numerical scheme for solving the FiSAC problem (1.1)-(1.3). This is done by using the finite difference method described above together with the standard first-order implicit-explicit (linear) scheme or the second-order Crank-Nicolson (nonlinear) scheme in time. More precisely, we have

$$\frac{U^{n+1} - U^n}{\tau} + ((U^n)^{\cdot 3} - U^n) = \epsilon^2 D_h U^{n+1} \quad (2.13)$$

and

$$\frac{U^{n+1} - U^n}{\tau} + \frac{(U^{n+1})^{\cdot 3} - U^{n+1}}{2} + \frac{(U^n)^{\cdot 3} - U^n}{2} = \frac{\epsilon^2 (D_h U^{n+1} + D_h U^n)}{2}, \quad (2.14)$$

where τ denotes the time stepsize, U^n represents the vector of numerical solution, and

$$(U^n)^{\cdot 3} := ((U_1^n)^3, (U_2^n)^3, \dots, (U_N^n)^3)^T.$$

In the sense of the truncation error, the approximation (2.13) is of order $O(\tau + h^2)$ and (2.14) is of order $O(\tau^2 + h^2)$.

3 The discrete maximum principle

To bound the numerical solutions, we first prove two useful lemmas.

Lemma 1. *If $D_h^{(d)}$, $d = 1, 2, 3$, is the discrete matrix defined in (2.10)-(2.12). Then $D_h = D_h^{(d)}$ satisfies the following properties:*

- D_h is symmetric;
- D_h is negative definite, i.e. $U^T D_h U < 0$, for any $U \in \mathbf{R}^N$;
- The elements of $D_h = (b_{ij})$ satisfy:

$$b_{ii} = -b < 0 \quad \text{and} \quad b \geq \max_i \sum_{j \neq i} |b_{ij}|. \quad (3.1)$$

Proof. From the definitions (2.10)-(2.12), it is obvious that if D in (2.9) satisfies the three properties above so does D_h . Consequently, we only need to check whether D satisfies the three properties. First, it follows from the definition $D = M + M^T$ that D is symmetric. Moreover, it can be easily

verified that $D = (d_{ij})$ is of the form

$$D = \begin{bmatrix} 2\omega_1^{(\alpha)} & \omega_0^{(\alpha)} + \omega_2^{(\alpha)} & \dots & \omega_{N-1}^{(\alpha)} & \omega_N^{(\alpha)} \\ \omega_0^{(\alpha)} + \omega_2^{(\alpha)} & 2\omega_1^{(\alpha)} & \omega_0^{(\alpha)} + \omega_2^{(\alpha)} & \dots & \omega_{N-1}^{(\alpha)} \\ \vdots & \omega_0^{(\alpha)} + \omega_2^{(\alpha)} & 2\omega_1^{(\alpha)} & \ddots & \vdots \\ \omega_{N-1}^{(\alpha)} & \dots & \ddots & \ddots & \omega_0^{(\alpha)} + \omega_2^{(\alpha)} \\ \omega_N^{(\alpha)} & \omega_{N-1}^{(\alpha)} & \dots & \omega_0^{(\alpha)} + \omega_2^{(\alpha)} & 2\omega_1^{(\alpha)} \end{bmatrix}_{N \times N}. \quad (3.2)$$

Since $1 < \alpha \leq 2$, we have

$$d_{ii} = 2\omega_1^{(\alpha)} = 2 - \alpha - \alpha^2 \leq 0. \quad (3.3)$$

Observe that

$$\omega_0^{(\alpha)} + \omega_2^{(\alpha)} = \frac{\alpha}{2} + \frac{\alpha(\alpha^2 + \alpha - 4)}{4} = \frac{\alpha(\alpha^2 + \alpha - 2)}{4} \geq 0$$

and $\omega_3^{(\alpha)} \geq \omega_4^{(\alpha)} \geq \dots \geq 0$. We then obtain that $d_{ij} \geq 0$, $i \neq j$. Furthermore, it follows from (2.8) that

$$\begin{aligned} -\omega_1^{(\alpha)} &> \omega_0^{(\alpha)} + \sum_{k=2}^N \omega_k^{(\alpha)} && \text{for } 1 < \alpha < 2, \\ -\omega_1^{(\alpha)} &= \omega_0^{(\alpha)} + \sum_{k=2}^{\infty} \omega_k^{(\alpha)} && \text{for } \alpha = 2. \end{aligned}$$

Consequently,

$$-d_{ii} = -2\omega_1^{(\alpha)} \geq 2\omega_0^{(\alpha)} + 2 \sum_{k=2}^N \omega_k^{(\alpha)} \geq \max_i \sum_{i \neq j} d_{ij} = \max_i \sum_{i \neq j} |d_{ij}|. \quad (3.4)$$

This verifies (3.1), which implies that D is negative diagonally dominated and hence negative definite.

This completes the proof. \square

Lemma 2. *Let B be a real $N \times N$ matrix and $A = aI - B$ with $a > 0$. If $B = (b_{ij})$ satisfies (3.1), then*

$$\|A\mathbf{v}\|_{\infty} \geq a\|\mathbf{v}\|_{\infty}, \quad \|A\mathbf{v} + c(\mathbf{v})^3\|_{\infty} \geq a\|\mathbf{v}\|_{\infty} + c\|\mathbf{v}\|_{\infty}^3, \quad (3.5)$$

where $c > 0$ and $\mathbf{v} \in \mathbf{R}^N$.

Proof. Suppose $\|\mathbf{v}\|_{\infty} = |v_p|$. Then $|v_p| \geq |v_j|$ for all $1 \leq j \leq N$. To simplify the notation, denote

$$\mathbf{s} = A\mathbf{v}, \quad \mathbf{t} = A\mathbf{v} + c(\mathbf{v})^3. \quad (3.6)$$

Then the p th components of \mathbf{s} and \mathbf{t} are

$$s_p = av_p - \sum_{j=1}^N b_{pj}v_j, \quad t_p = av_p + cv_p^3 - \sum_{j=1}^N b_{pj}v_j. \quad (3.7)$$

Obviously, av_p and cv_p^3 have same signs. Next we will check both av_p and $-\sum_{j=1}^N b_{pj}v_j$ have the same sign. This can be verified by

$$\begin{aligned} av_p \cdot \left(-\sum_{j=1}^N b_{pj}v_j \right) &= av_p \left(-b_{pp}v_p - \sum_{j \neq p} b_{pj}v_j \right) = a \left(bv_p^2 - \sum_{j \neq p} b_{pj}v_jv_p \right) \\ &\geq a \left(b|v_p|^2 - \sum_{j \neq p} |b_{pj}||v_j||v_p| \right) \geq a \left(b|v_p|^2 - \sum_{j \neq p} |b_{pj}||v_p|^2 \right) \\ &\geq a \left(b - \sum_{j \neq p} |b_{pj}| \right) |v_p|^2 \geq 0. \end{aligned} \quad (3.8)$$

Therefore av_p , cv_p^3 and $-\sum_{j=1}^N b_{pj}v_j$ are positive or negative simultaneously. Consequently,

$$|s_p| \geq a|v_p| = a\|\mathbf{v}\|_\infty, \quad |t_p| \geq a|v_p| + c|v_p|^3 = a\|\mathbf{v}\|_\infty + c\|\mathbf{v}\|_\infty^3. \quad (3.9)$$

Using the facts $\|\mathbf{s}\|_\infty \geq |s_p|$ and $\|\mathbf{t}\|_\infty \geq |t_p|$ yields the desired estimates (3.5). \square

Theorem 1. *Assume the initial value satisfies $\max_{\mathbf{x} \in \Omega} |u_0(\mathbf{x})| \leq 1$. Then the fully discrete scheme (2.13) preserves the maximum principle in the sense that $\|U^n\|_\infty \leq 1$ for all $n \geq 1$ provided that the time stepsize satisfies $0 < \tau \leq \frac{1}{2}$.*

Proof. We prove this theorem by induction. First it follows from the assumption on u_0 that $\|U^0\|_\infty \leq 1$. We now assume that the result holds for $n = m$ i.e. $\|U^m\|_\infty \leq 1$. Below we will check this upper bound is also true for $n = m + 1$. It follows from the linear scheme (2.13) that

$$(I - \tau\epsilon^2 D_h)U^{m+1} = U^m + \tau(U^m - (U^m)^3). \quad (3.10)$$

Since $\tau\epsilon^2 D_h$ satisfies the properties in Lemma 1, it follows from Lemma 2 that

$$\|(I - \tau\epsilon^2 D_h)U^{m+1}\|_\infty \geq \|U^{m+1}\|_\infty. \quad (3.11)$$

Observe that each element of $U^m + \tau(U^m - (U^m)^3)$ is of the form

$$g(x) = x + \tau(x - x^3). \quad (3.12)$$

It can be verified that $g'(x) = \tau\left(\frac{1}{\tau} + 1 - 3x^2\right) \geq 0$ for $x \in [-1, 1]$ provided that $0 < \tau \leq \frac{1}{2}$.

Consequently

$$\max_{|x| \leq 1} g(x) = g(1) = 1; \quad \min_{|x| \leq 1} g(x) = g(-1) = -1,$$

which implies that $|g(x)| \leq 1$ for $|x| \leq 1$. As a result, we conclude $\|U^m + \tau(U^m - (U^m)^3)\|_\infty \leq 1$ if $\|U^m\|_\infty \leq 1$. This, together with (3.10) and (3.11), completes the induction, and the proof of this theorem is ended. \square

Theorem 2. *Assume the initial value satisfies $\max_{\mathbf{x} \in \Omega} |u_0(\mathbf{x})| \leq 1$. Then the fully discrete scheme (2.14) preserves the maximum principle in the sense that $\|U^n\|_\infty \leq 1$ for all $n \geq 1$ provided that the time stepsize satisfies*

$$0 < \tau \leq \min \left\{ \frac{1}{2}, \frac{h^\alpha}{2d\epsilon^2} \right\}, \quad (3.13)$$

where d is the dimension number.

Proof. Again we will prove this theorem by induction. It follows from the scheme (2.14) that

$$\left(1 - \frac{\tau}{2}\right) U^{m+1} + \frac{\tau}{2} (U^{m+1})^3 - \frac{\tau\epsilon^2}{2} D_h U^{m+1} = \left(I + \frac{\tau\epsilon^2}{2} D_h\right) U^m + \frac{\tau}{2} (U^m - (U^m)^3). \quad (3.14)$$

By Lemma 2, we have

$$\left\| \left(1 - \frac{\tau}{2}\right) U^{m+1} + \frac{\tau}{2} (U^{m+1})^3 - \frac{\tau\epsilon^2}{2} D_h U^{m+1} \right\|_\infty \geq \left(1 - \frac{\tau}{2}\right) \|U^{m+1}\|_\infty + \frac{\tau}{2} \|U^{m+1}\|_\infty^3. \quad (3.15)$$

Let $H = \frac{1}{2}I + \frac{\tau\epsilon^2}{2} D_h$. Then

$$\left(I + \frac{\tau\epsilon^2}{2} D_h\right) U^m + \frac{\tau}{2} (U^m - (U^m)^3) = H U^m + \frac{U^m + \tau(U^m - (U^m)^3)}{2}. \quad (3.16)$$

It is easy to verify that the matrix $H = (h_{ij})$ in the d -dimension satisfies

$$i) \ h_{ii} = \frac{1}{2} - \frac{d\tau\epsilon^2(\alpha^2 + \alpha - 2)}{4h^\alpha(-\cos\frac{\pi}{2}\alpha)}, \quad ii) \ h_{ij}|_{j \neq i} \geq 0 \quad \text{and} \quad \max_i \sum_j h_{ij} \leq \frac{1}{2}. \quad (3.17)$$

If we assume $h_{ii} \geq 0$, i.e.,

$$\tau \leq \frac{2h^\alpha(-\cos\frac{\pi}{2}\alpha)}{d\epsilon^2(\alpha^2 + \alpha - 2)}, \quad (3.18)$$

then H is non-negative, i.e., $h_{ij} \geq 0$ for $1 \leq i, j \leq N$. Consequently,

$$\|H\|_\infty = \max_i \sum_j |h_{ij}| = \max_i \sum_j h_{ij} \leq \frac{1}{2}. \quad (3.19)$$

We further denote

$$p(\alpha) := \frac{-\cos \frac{\pi}{2}\alpha}{\alpha^2 + \alpha - 2}. \quad (3.20)$$

It is easy to verify that

$$\frac{1}{4} < p(\alpha) < \frac{\pi}{6}, \quad \text{for } \alpha \in (1, 2). \quad (3.21)$$

This allows us to simplify the constraint imposed on time step (3.18) as

$$\tau \leq \frac{h^\alpha}{2d\epsilon^2}. \quad (3.22)$$

Now consider the last term of (3.16). If $\|U^m\|_\infty \leq 1$, using the argument for $g(x)$ in the proof of Theorem 1 gives

$$\|U^m + \tau (U^m - (U^m)^3)\|_\infty \leq 1, \quad 0 < \tau \leq \frac{1}{2}. \quad (3.23)$$

If $\|U^m\|_\infty \leq 1$, then combining (3.19) and (3.23) yields

$$\begin{aligned} & \left\| \left(I + \frac{\tau\epsilon^2}{2} D_h \right) U^m + \frac{\tau}{2} (U^m - (U^m)^3) \right\|_\infty \\ &= \left\| H U^m + \frac{U^m + \tau (U^m - (U^m)^3)}{2} \right\|_\infty \\ &\leq \|H\|_\infty \|U^m\|_\infty + \frac{1}{2} \|U^m + \tau (U^m - (U^m)^3)\|_\infty \leq \frac{1}{2} + \frac{1}{2} = 1, \end{aligned} \quad (3.24)$$

provided that the condition (3.13) is satisfied. Consequently, using (3.15) gives

$$\left(1 - \frac{\tau}{2}\right) \|U^{m+1}\|_\infty + \frac{\tau}{2} \|U^{m+1}\|_\infty^3 \leq 1, \quad (3.25)$$

which yields $\|U^{m+1}\|_\infty \leq 1$. This completes the proof of Theorem 2. \square

4 The discrete energy stability

After being semi-discretized in space, an ODE system is obtained

$$\frac{dU}{dt} = \epsilon^2 D_h U + U - U^3, \quad (4.1)$$

where D_h is given by (2.10)-(2.12) for one to three space dimensions, respectively. If we define the following discrete energy:

$$E_h(U) = \frac{1}{4} \sum_{i=1}^N (U_i^2 - 1)^2 - \frac{\epsilon^2}{2} U^T D_h U, \quad (4.2)$$

then the ODE system (4.1) can be viewed as the gradient flow of the energy $E_h(U)$, i.e.,

$$\frac{dU}{dt} = -\nabla_U E_h(U). \quad (4.3)$$

Taking L^2 inner product of (4.3) with $-\frac{dU}{dt}$ yields

$$\frac{dE_h(U)}{dt} = -\left\| \frac{dU}{dt} \right\|_2^2 \leq 0, \quad (4.4)$$

which implies that the energy $E_h(U)$ defined by (4.2) decays with time. Our next task is to show that this energy stability can be inherited by both the first-order scheme (2.13) and the second-order scheme (2.14).

Theorem 3. *Under the conditions in Theorem 1, the numerical solutions obtained by the scheme (2.13) can guarantee the discrete energy decay properly, i.e.,*

$$E_h(U^{n+1}) \leq E_h(U^n), \text{ for } n = 0, 1, 2, \dots. \quad (4.5)$$

Proof. Taking the difference of the discrete energy between two time level, we get

$$\begin{aligned} & E_h(U^{n+1}) - E_h(U^n) \\ &= \frac{1}{4} \sum_{i=1}^N \left[\left((U_i^{n+1})^2 - 1 \right)^2 - \left((U_i^n)^2 - 1 \right)^2 \right] - \frac{\epsilon^2}{2} \left((U^{n+1})^T D_h U^{n+1} - (U^n)^T D_h U^n \right). \end{aligned} \quad (4.6)$$

Taking L^2 inner product of (2.13) with $(U^{n+1} - U^n)^T$ obtains

$$\sum_{i=1}^N \left[\left((U_i^n)^3 - U_i^n \right) (U_i^{n+1} - U_i^n) + \frac{1}{\tau} (U_i^{n+1} - U_i^n)^2 \right] - \epsilon^2 (U^{n+1} - U^n)^T D_h U^{n+1} = 0. \quad (4.7)$$

Since the discrete Laplace operator D_h is symmetric, we have

$$\begin{aligned} & (U^{n+1} - U^n)^T D_h U^{n+1} \\ &= \frac{1}{2} \left((U^{n+1})^T D_h U^{n+1} - (U^n)^T D_h U^n \right) + \frac{1}{2} (U^{n+1} - U^n)^T D_h (U^{n+1} - U^n). \end{aligned} \quad (4.8)$$

Note that for all $a, b \in [-1, 1]$

$$(b^3 - b)(a - b) + (a - b)^2 \geq \frac{1}{4} \left[(a^2 - 1)^2 - (b^2 - 1)^2 \right]. \quad (4.9)$$

Under the conditions in Theorem 1, we have $\|U^{n+1}\|_\infty \leq 1$ and $\|U^n\|_\infty \leq 1$. Consequently, combining this with (4.6)-(4.9) gives

$$\begin{aligned} & E_h(U^{n+1}) - E_h(U^n) \\ & \leq \frac{\epsilon^2}{2} (U^{n+1} - U^n)^T D_h (U^{n+1} - U^n) + \left(1 - \frac{1}{\tau} \right) \sum_{i=1}^N (U_i^{n+1} - U_i^n)^2. \end{aligned} \quad (4.10)$$

As D_h is a negative definite matrix and $0 < \tau \leq \frac{1}{2}$, the desired result follows from the above inequality. \square

Theorem 4. *Under the conditions in Theorem 2, the numerical solutions obtained by the scheme (2.14) can guarantee the discrete energy decay properly, i.e.,*

$$E_h(U^{n+1}) \leq E_h(U^n), \text{ for } n = 0, 1, 2, \dots. \quad (4.11)$$

Proof. Taking L^2 inner product of (2.14) with $(U^{n+1} - U^n)^T$ obtains

$$\begin{aligned} & \sum_{i=1}^N \left[\frac{1}{2} \left((U_i^{n+1})^3 - U_i^{n+1} \right) (U_i^{n+1} - U_i^n) + \frac{1}{2} \left((U_i^n)^3 - U_i^n \right) (U_i^{n+1} - U_i^n) + \frac{1}{\tau} (U_i^{n+1} - U_i^n)^2 \right] \\ &= \frac{\epsilon^2}{2} (U^{n+1} - U^n)^T D_h (U^{n+1} + U^n). \end{aligned} \quad (4.12)$$

Since the discrete Laplace operator D_h is symmetric, we have

$$\frac{\epsilon^2}{2} (U^{n+1} - U^n)^T D_h (U^{n+1} + U^n) = \frac{\epsilon^2}{2} \left((U^{n+1})^T D_h U^{n+1} - (U^n)^T D_h U^n \right). \quad (4.13)$$

Note that for any $a, b \in \mathbf{R}$

$$(a^3 - a)(a - b) + (a - b)^2 \geq \frac{1}{4} \left[(a^2 - 1)^2 - (b^2 - 1)^2 \right]. \quad (4.14)$$

Under the conditions in Theorem 2, we have $\|U^{n+1}\|_\infty \leq 1$ and $\|U^n\|_\infty \leq 1$. Consequently, it follows from (4.9) and (4.14) that

$$\begin{aligned} & \frac{1}{4} \sum_{i=1}^N \left[\left((U_i^{n+1})^2 - 1 \right)^2 - \left((U_i^n)^2 - 1 \right)^2 \right] \\ & \leq \sum_{i=1}^N \left[\frac{1}{2} \left((U_i^{n+1})^3 - U_i^{n+1} \right) (U_i^{n+1} - U_i^n) + \frac{1}{2} \left((U_i^n)^3 - U_i^n \right) (U_i^{n+1} - U_i^n) + (U_i^{n+1} - U_i^n)^2 \right]. \end{aligned} \quad (4.15)$$

This together with (4.6) and (4.12)-(4.13), yield

$$E_h(U^{n+1}) - E_h(U^n) \leq \left(1 - \frac{1}{\tau} \right) \sum_{i=1}^N (U_i^{n+1} - U_i^n)^2. \quad (4.16)$$

Since $0 < \tau \leq \frac{1}{2}$, the right-hand side of (4.16) is non-positive,

$$E_h(U^{n+1}) - E_h(U^n) \leq 0, \quad (4.17)$$

which implies that (4.11) holds. \square

We close this section by pointing out that although the above energy stability result for the Crank-Nicolson scheme is conditional, our numerical experiments show that the condition (3.13) may be removed, i.e., the energy stability may be unconditional. It is noted Qiao et al. [13] obtained a unconditional energy stability result for the Crank-Nicolson approximation for a relevant phase-field model.

5 Numerical Results

In this section, we present a number of numerical experiments to verify the theoretical results obtained in the previous sections. We consider the one-dimensional FiSAC equation in the first two examples and two-dimensional problem in the third example.

Example 1. *This example uses the first order scheme (2.13) with the initial value*

$$u_0(x) = \begin{cases} \frac{\sqrt{3}}{2} - 200\sqrt{3}(x - 0.05)^2, & 0 \leq x \leq 0.05, \\ \frac{\sqrt{3}}{2}, & 0.05 < x < 0.95, \\ \frac{\sqrt{3}}{2} - 200\sqrt{3}(x - 0.95)^2, & 0.95 \leq x \leq 1. \end{cases}$$

The mesh size in space is fixed as $h = 0.01$, and the time step τ and the fractional derivative parameter α are varied. For the first-order implicit-explicit scheme (2.13) with $\alpha = 1.5$ and the parameter $\epsilon = 0.01$, it can be observed from Fig. 1 that the discrete maximum principle is preserved for $\tau = 0.5$. However, the maximum value exceeds 1 for $\tau > 0.5$, such as $\tau = 1$ and 1.5. This result is consistent with the theoretical prediction of Theorem 1. With the same parameters setting, we plot the energy curve and observe that the energy decay property does not hold for $\tau > 0.5$. This result is consistent with the prediction of Theorem 2.

In Fig. 2, we choose $\tau = 0.01$ and $\epsilon = 0.2$ and plot the numerical solutions at $t = 20$ with different fractional parameters α . It is observed that the numerical solutions become more gentle when α varies from 2 to 1.1.

Example 2. *The second example is concerned with the second-order scheme (2.14) with $\alpha = 1.5$. The following initial condition is used*

$$u_0(x) = 0.95 \times \text{rand}(\cdot) + 0.05,$$

where $\text{rand}(\cdot)$ represents a random number on each point in $(0, 1)$, and zero boundary values are set for $u_0(x)$.

We fix the mesh size in space as $h = 0.1$ and the nonlinear equation (2.14) is solved by Newton's iteration method which turns out to be very efficient. Note the initial guess at each Newton iteration is obtained by using the linear scheme (2.13). It is observed that the maximum principle is indeed decided by the condition (3.13). To explain this more clearly, we denote $\theta = \frac{h^\alpha}{2d\epsilon^2}$. For the case $\epsilon = 0.1$ (recall $h = 0.1$), we have $\theta \approx 1.581$, which implies that the condition (3.13) becomes $\tau \leq 0.5$. In the top two sub-figures of Fig. 3, the maximum value of numerical solution is bounded by 1 for $\tau = 0.4$ and exceeds 1 if $\tau = 1.5$. If we change ϵ to be 0.9, then we obtain $\theta \approx 0.0195$, which implies that the condition (3.13) becomes $\tau \leq 0.0195$. Indeed we observe that the maximum value is preserved if $\tau = 0.01$ and is not preserved if $\tau = 0.4$.

Example 3. Consider the first order scheme (2.13) with following initial value in two-space dimension:

$$u_0(x, y) = 0.1 \times \text{rand}(\cdot) - 0.05,$$

where $\text{rand}(\cdot)$ represents a random number on each point in $(0, 1)^2$. Zero boundary value is set for $u_0(x, y)$.

We fix $\alpha = 1.5$, $\epsilon = 0.02$ and $h_x = h_y = 0.01$, while the time step τ will be varied. Fig. 4 shows the numerical results and the energy curve, and it is found that similar behaviors for Example 1 are observed.

In Fig. 5, we investigate the effects of fractional diffusion when spinodal decomposition is considered. For $\alpha = 2$ the early stages of phase transition produce a rapid movement to bulk regions of both phases and then motion slows down resulting in the state given at times $t = 25, 50, 100$, respectively. Reducing the fractional power leads to thinner interfaces that allow for smaller bulk regions and a much more heterogeneous phase structure. Furthermore, motion to large bulk regions is dramatically slowed down for fractional models with $\alpha = 1.1, 1.4, 1.7$. This phenomenon is consistent with the finding of [2].

6 Conclusions

The main contribution of this work is the establishment of the maximum norm stability for the discrete fractional-in-space Allen-Cahn equation. The result is obtained under a framework which is independent of the space dimension. Under this framework we are also able to recover the energy decaying property for the Crank-Nicolson time discretization approximation under certain restrictions on time steps. However, numerical experiments suggest that this energy stability may be unconditional, which remains to be better understood by some refined analysis.

7 Acknowledgments

The research of the first author is supported by China Postdoctoral Science Foundation funded project (2013M542188). The research of the second author is supported in part by Hong Kong Research Grants Council CERG grants, National Science Foundation of China, and Hong Kong Baptist University FRG grants. The third author is supported by Hong Kong Research Grants Council and Hong Kong Baptist University.

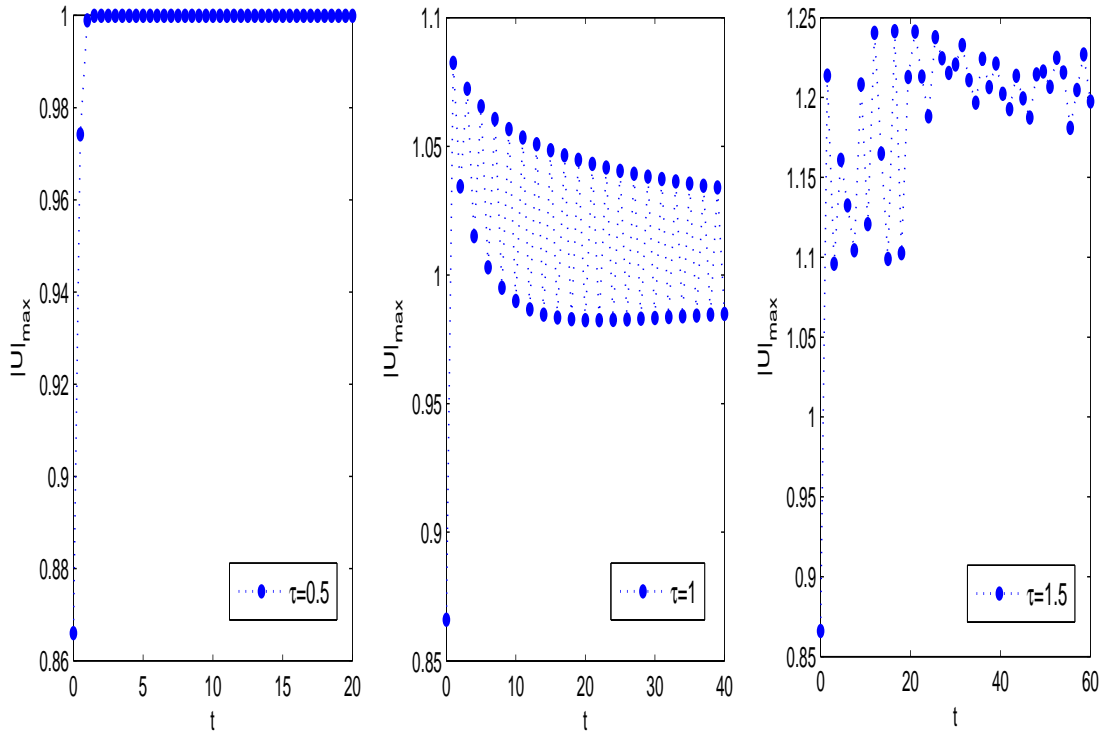
References

- [1] S.M. Allen and J.W. Cahn, A microscopic theory for antiphase boundary motion and its application to antiphase domain coarsening, *Acta Metall*, **27** (1979), 1085-1095.
- [2] K. Burrage, N. Hale and D. Kay, An efficient implicit FEM scheme for fractional-in-space reaction-diffusion equations, *SIAM J. Sci. Comput*, **34** (2012), A2145-A2172.
- [3] J. W. Choi, H. G. Lee, D. Jeong , et al. An unconditionally gradient stable numerical method for solving the Allen-Cahn equation, *Physica A: Statistical Mechanics and its Applications*, **388**(9) (2009) 1791-1803.
- [4] D.J. Eyre, An unconditionally stable one-step scheme for gradient systems. June 1998, unpublished. <http://www.math.utah.edu/eyre/research/methods/stable.ps>.

- [5] X. Feng and A. Prohl, Numerical analysis of the Allen-Cahn equation and approximation for mean curvature flows, *Numer. Math.*, 94(1) (2003), 33-65.
- [6] X. Feng, H. Song, T. Tang and J. Yang, Nonlinearly stable implicit-explicit methods for the Allen-Cahn equation. Preprint.
- [7] X. Feng, T. Tang and J. Yang, Stabilized Crank-Nicolson/Adams-Bashforth schemes for phase field models, *East Asian Journal on Applied Mathematics*, 3 (2013), 59-80.
- [8] J. Kim, Phase-field models for multi-component fluid flows, *Commun. Comput. Phys*, 12 (2012), 613-661.
- [9] T. A. M. Langlands and B. I. Henry, The accuracy and stability of an implicit solution method for the fractional diffusion equation, *J. Comp. Phys*, 205 (2005), 719-736.
- [10] X. J. Li and C. J. Xu, A space-time spectral method for the time fractional diffusion equation, *SIAM J. Numer. Anal*, 47(3) (2009), 2108-2131.
- [11] Y. M. Lin and C. J. Xu, Finite difference/spectral approximations for the time-fractional diffusion equation, *J. Comput. Phys*, 225 (2007), 1533-1552.
- [12] A. Bueno-Orovio, D. Kay and K. Burrage, Fourier spectral methods for fractional-in-space reaction-diffusion equations, *J. Comp. Phy*, submitted.
- [13] Z.H. Qiao, Z.R. Zhang and T. Tang, An adaptive time-stepping strategy for the molecular beam epitaxy models, *SIAM J. Sci. Comput.*, **33** (2011), 1395-1414.
- [14] J. Shen and X. Yang, Numerical approximations of Allen-Cahn and Cahn-Hilliard equations, *Discret. Contin. Dyn. Syst.* , **28** (2010), 1669-1691.
- [15] W. Tian, H. Zhou and W. Deng, A class of second order difference approximations for solving space fractional diffusion equations. Preprint.
- [16] T. Tang and J. Yang, Implicit-explicit scheme for the Allen-Cahn equation preserves the maximum Principle. Preprint.
- [17] X. Yang, Error analysis of stabilized semi-implicit method of Allen-Cahn equation, *Discrete Contin. Dyn. Syst. Ser. B*, 11(4) (2009) 1057-1070.

- [18] S. B. Yuste and L. Acedo, An explicit finite difference method and a new Von Neumann-type stability analysis for fractional diffusion equations, *SIAM J. Numer. Anal.*, 42 (2005), 1862-1874.
- [19] J. Zhang and Q. Du, Numerical studies of discrete approximations to the Allen-Cahn equation in the sharp interface limit, *SIAM J. Sci. Comput.*, 31(4) (2009) 3042-3063.
- [20] P. Zhuang, F. Liu, V. Anh and I. Turner, Numerical methods for the variable-order fractional advection-diffusion equation with a nonlinear source term, *SIAM J. Numer. Anal.*, 47 (2009), 1760-1781.

(a)



(b)

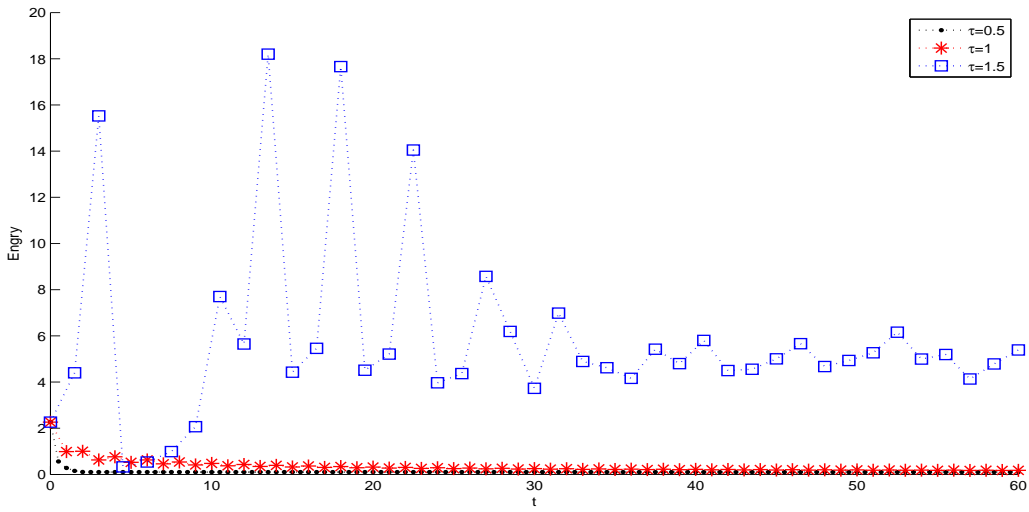


Figure 1: Example 1 with scheme (2.13): (a) the maximum values with different times steps ($\alpha = 1.5, \epsilon = 0.01$); (b) energy curve with different times steps ($\alpha = 1.5, \epsilon = 0.01$).

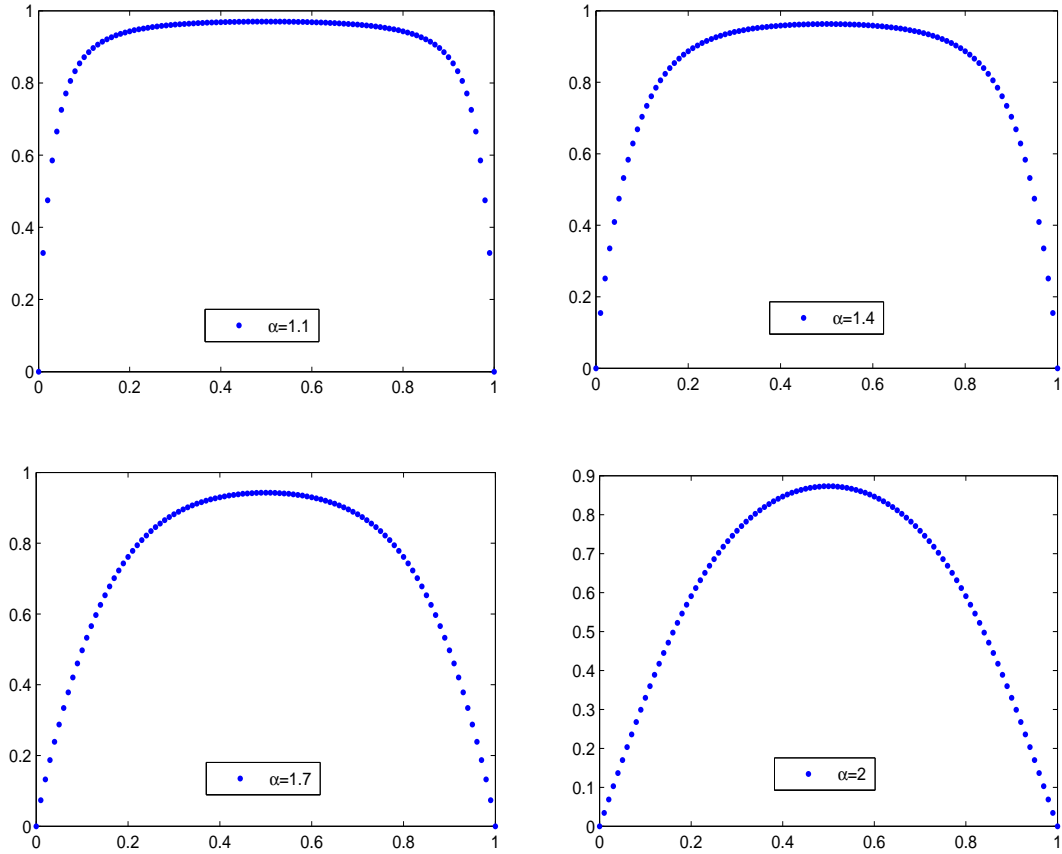


Figure 2: Example 1 with scheme (2.13): numerical solutions at $t = 20$ with different values of α ($\tau = 0.01, \epsilon = 0.2$).

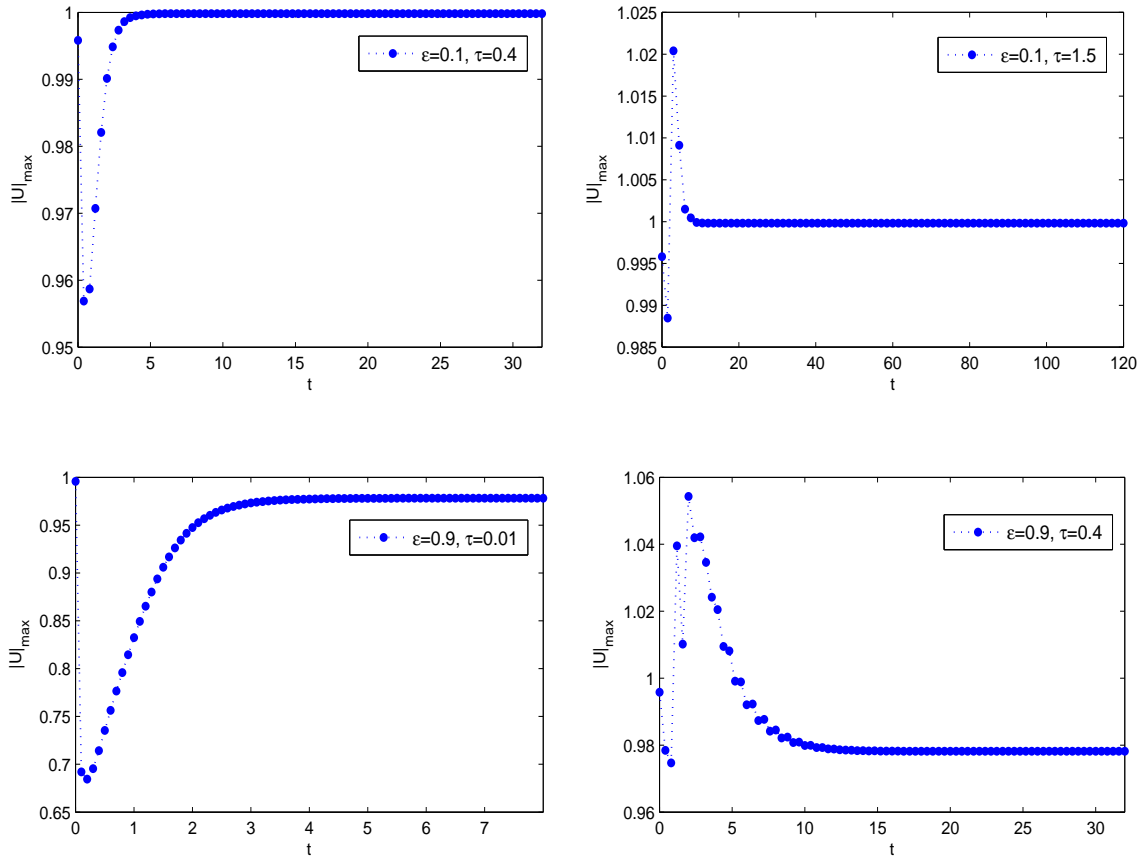
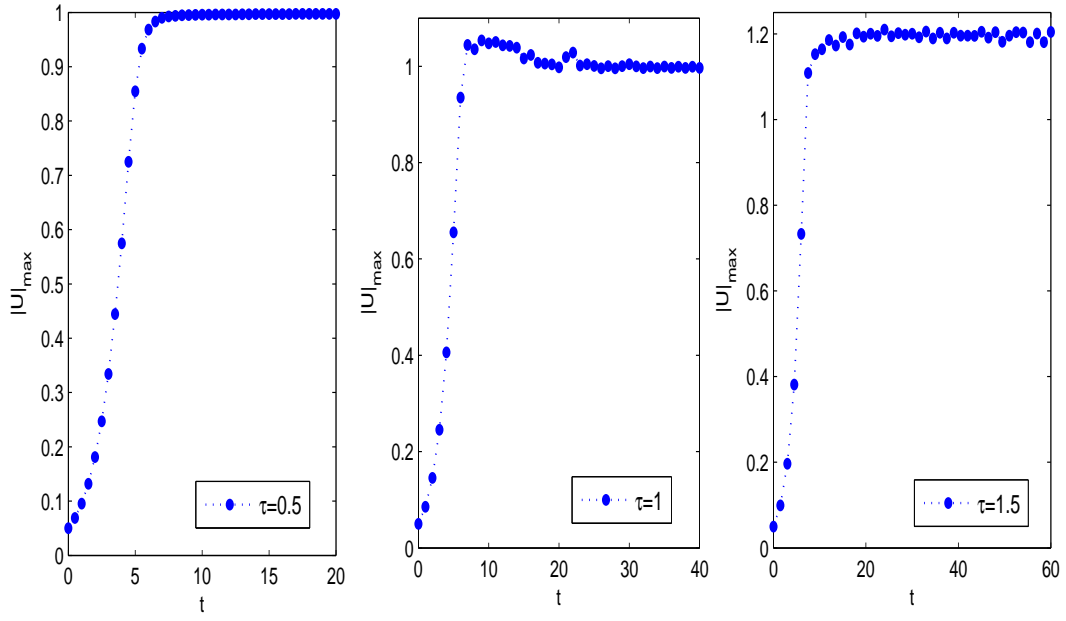


Figure 3: Example 2 with $\alpha = 1.5$ and $h = 0.1$: the numerical solutions for the scheme (2.14) with different ϵ and τ .

(a)



(b)

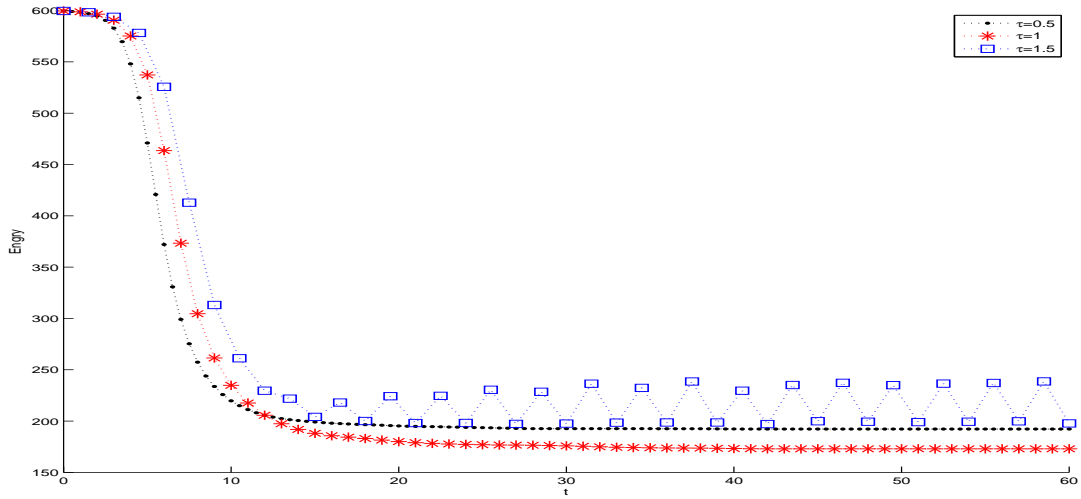


Figure 4: Example 3 with the second-order scheme (2.13): (a) numerical solutions; and (b) energy curve. $\alpha = 1.5$ and $\epsilon = 0.02$, with different time steps $\tau = 0.5, 1, 1.5$.

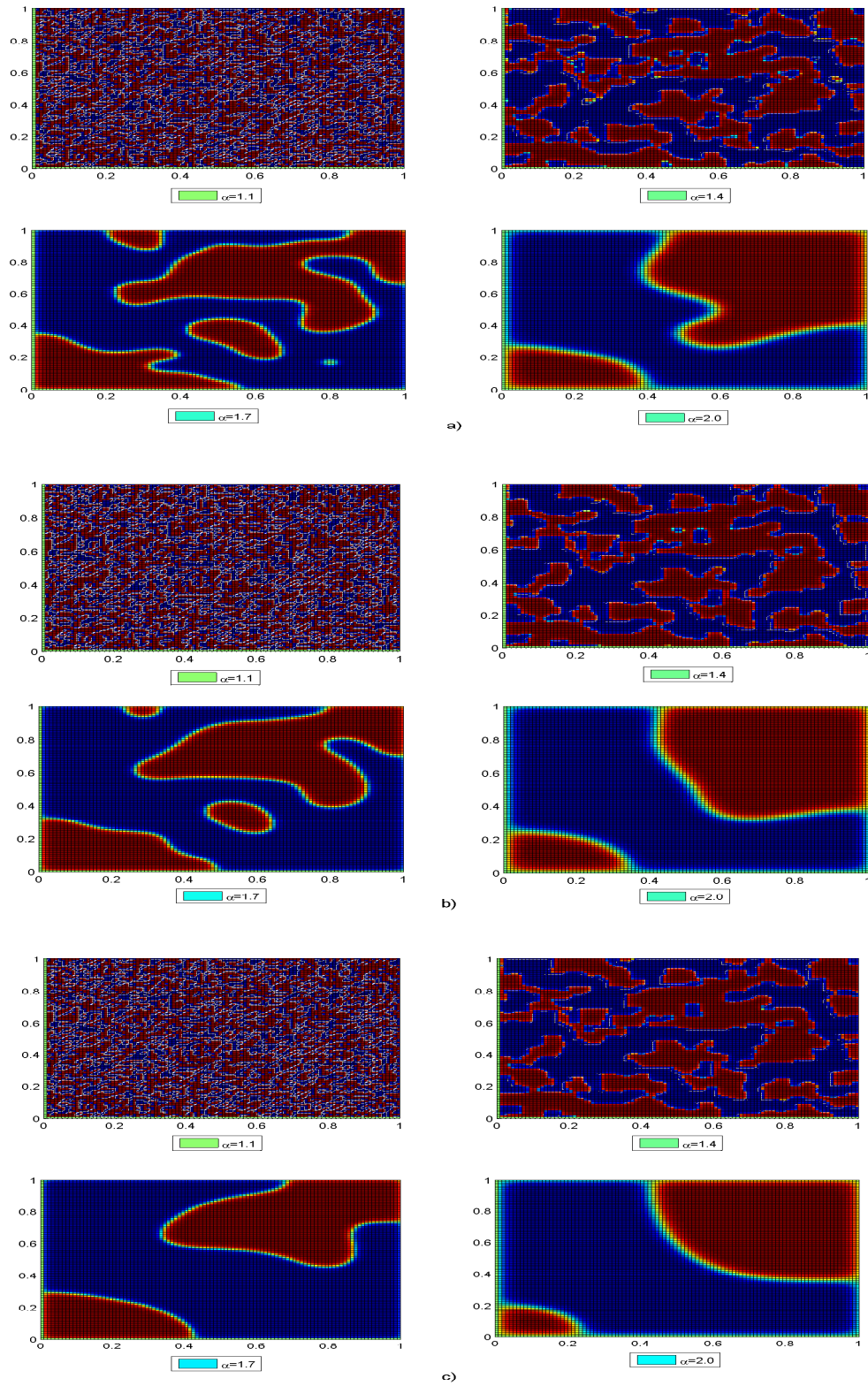


Figure 5: Example 3. Numerical solutions at a) $t = 25$, b) $t = 50$ and c) $t = 100$ with different fractional derivatives $\alpha = 1.1, 1.4, 1.7, 2$.